Instrumentation for Measuring Bioelectrical Signals in Plants

L. KARLSSON

Physics Laboratory, Royal Veterinary and Agricultural University, Copenhagen, Denmark

(Received 27 August 1971; and in final form, 22 October 1971)

An electronic instrumentation for the measurement of bioelectrical signals in plants is presented. The problems of common mode signal rejection and amplifier bias current are considered. With the instrumentation presented recordings have been made of bioelectrical signals generated in the India rubber tree (*Ficus elastica*).

INTRODUCTION

The basic source of all bioelectrical potentials is the cell. According to convention, the cell bioelectrical potential, or transmembrane potential, is defined as the difference in potential between the inside and the outside of the cell membrane. In order to measure electrical effects in plant tissue it is necessary to make a conversion from the ionic conduction, present in the tissue, to the electronic conduction which occurs in the measuring circuit. This conversion is accomplished at the tissue–electrode interface.

Two distinct classes of cell bioelectrical potential measurements exist. The intracellular action potential is measured with one electrode placed inside a cell while the reference electrode is situated in the conducting medium surrounding the cell. The extracellular action potential is measured with both electrodes in contact with the conducting tissue embodying larger groups of cells. In the latter case the signal observed is due to the depolarization–repolarization process in a group of cells. Because of the tissue and cell membrane impedances, the external action potential that is recorded is somewhat similar to a mathematical time derivative of the transmembrane potential. Abundant measurements of these two types have been made in animal electrophysiology. The well-known electrocardiographic (ECG) and electroencephalographic (EEG) methods are based upon measurements of the summed bioelectrical activity in large groups of cells.

The instrumentation described in the following has been made for the recording of nonevoked bioelectrical signals in plant tissue. Much of the technique used has been taken over from what is employed in EEG and ECG measurements. The results of these measurements on the India rubber tree are treated in more detail elsewhere.[1] To the best of the author's knowledge no such measurements have been reported on before.

In almost all physiological measurement situations, at least two signals are present: The desired bioelectrical signal and an interference signal at the line voltage frequency. The latter signal, which can be much larger in amplitude than the desired signal, is produced by the plant or animal due to electrostatically coupled and magnetically induced interference. The use of line-frequency rejection filters is generally avoided because this can lead to distortion of the physiological signal. By the use of a differential amplifier with high common mode rejection ratio, CMRR, it is normally possible to reject the line frequency interference signal to a satisfactory degree because this is largely a common mode signal. In order to make operative the CMRR available with a particular differential amplifier, the CMRR degrading due to unequal source impedances at the tissue–electrode interfaces should be considered carefully. An effective high CMRR in the frequency range of interest is especially important when recording unpredictable signals such that these shall not be confused by interference signals from sources external to the plant. During the present series of measurements, the electrical activity of two plants, placed close together, were recorded simultaneously. By this coincidence method external interference will mark itself by its presence in both recordings. Further, with the same objective, measurements were carried out with two amplifiers and associated electrodes connected to different parts of the same plant.

METHOD

The experimental setup for one channel consists in four basic units, a preamplifier with a differential input and a gain of 50, a linear bandpass amplifier with variable gain, a Y–T ink recorder, and an oscilloscope with storage capability. The bias current of the preamplifiers, to be "sinked" via the plant tissue, was considered a possible source of error, if it could trigger the plant cells.[2] In order to investigate the effect of the bias current on the signals observed, three amplifier types were made, types A, B, and C, the first with a bias current of 300 nA, type B with about 30 nA of bias current, and type C, a FET input type, with a bias current in the 5–200 pA range. To secure a relatively fast stabilization of the electrode–tissue offset potentials, a 2 MΩ resistor was inserted to limit the differential input resistance. The common mode input resistance is above 1000 MΩ in all three amplifier types.

The purpose of the linear bandpass amplifier is to pass only the frequency band of interest and hereby increase the signal-to-noise ratio. Simple 6 dB/octave RC and CR filters have been used to implement the bandpass operation. The amplifier has been designed with a gain variable from 1 to 500, because it was found that varying the

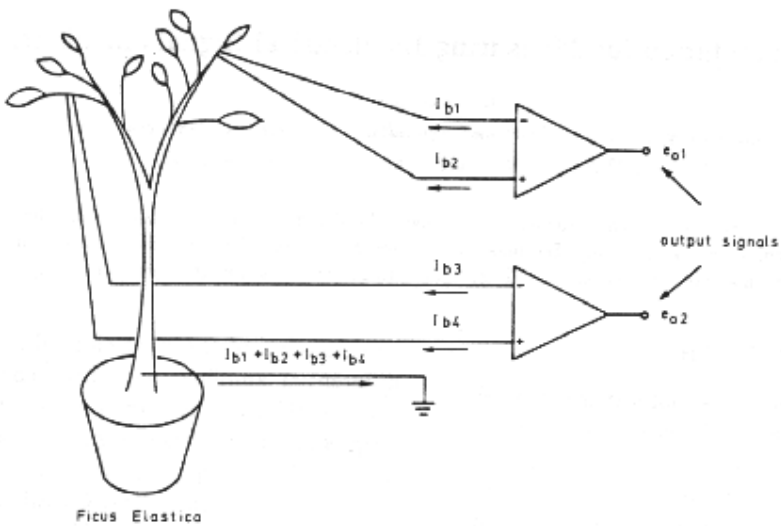

FIG. 1. Schematic drawing of the experimental setup.

sensitivity range on the Y–T ink recorders used, W+W type 2011, resulted in a variation of the frequency response and settling time of the recorder.

Because of the rather limited frequency response of the ink recorders, an oscilloscope with storage capability, a Tektronix type 549, was used to investigate the signals for higher frequency content. Also, AM and FM radios were used in order to discover any correlation between atmospheric and locally generated electrical noise and the signals generated in the plant.

An experimental setup in which two amplifiers are connected to different parts of the same plant is shown in Fig. 1. In this way the common mode interference signals in the two channels are made nearly identical and are thus easily identified.

The two preamplifiers were fed from a common stabilized ±15 V power supply. If any noise signals come via the power supply, this would manifest itself equally in the output signals from the preamplifiers and in this way be identified. Likewise, the two linear amplifiers were fed from a common stabilized power supply. The integrated circuit operational amplifiers used had a power supply rejection ratio, PSRR, of not less than 80 dB, which in itself ensures a high degree of immunity to power supply induced signals.

In Fig. 2 is shown a first order approximation equivalent circuit corresponding to the setup in Fig. 1. This circuit cannot strictly be referred to as an equivalent circuit as the electronic current flow in an electrical circuit and the ionic current flow present in the plant tissue cannot be said to be equivalent. A Thévenin equivalent circuit is shown, but the Norton equivalent could as well represent the setup. The networks and voltage generators enclosed by the dashed lines represent the electrode–tissue interfaces. The voltage generators $e_1,\cdots,e_5$ represent the offset potentials that exist at these interfaces. With 0.4 mm diam gold electrodes inserted into the petioles on the *Ficus elastica* plant these offset potentials were found to be in the 10–100 mV range. Long term differential drift of these potentials does not present any problem with the present instrumentation, when the dc gain used, before the first differentiation is performed, is limited to 50. The common mode interference signal, which is primarily 50 Hz line voltage induced, is represented by the e_{CM} voltage generator. In the case of an unshielded plant this signal can have amplitudes up to several volts depending on the local electrical environment. All conducting objects within 1–2 m from the plant must be securely connected to the common earth terminal in order to minimize the e_{CM} amplitude. The networks R_8C_8, R_9C_9, and $R_{10}C_{10}$ simulate the electrical behavior of the main body of the plant (cf. Fig. 1). Voltage generators e_6 and e_7 in connection with the R_6C_6 and R_7C_7 networks represent the bioelectrical signal sources.

From this equivalent circuit it can be concluded that it is desirable to use differential amplifiers with low bias currents and high input impedances. This excludes, at room temperature operation, all operational amplifiers except the FET-input category with bias currents in the 5–200 pA range. Good isolation between the e_6 and e_7 signal sources was observed with all three amplifier types (A, B, and C), but the stability of the offset potentials $e_1,\cdots,e_5$ increased with decreasing bias current. It was found that the differential mode noise generated at the electrode–tissue interfaces increased proportionally to the bias current supplied by the preamplifiers.

The best common mode rejection of line frequency signals was obtained when the reference electrode, which

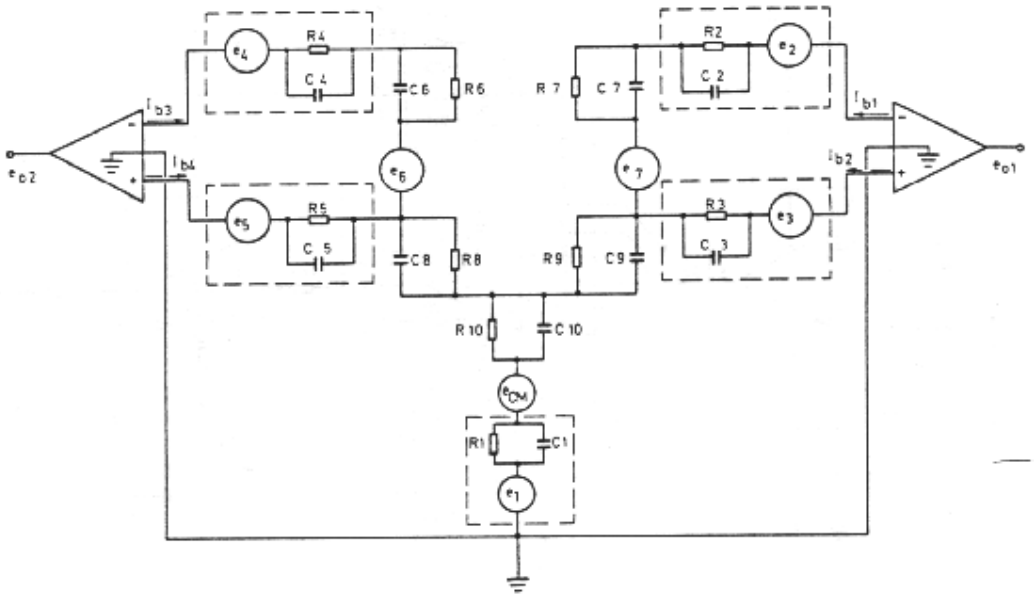

FIG. 2. A first order equivalent circuit representing the setup shown in Fig. 1.

is earthed at the preamplifier input, was placed far from the two measuring electrodes as indicated in Fig. 1.

CIRCUIT DESCRIPTION

The preamplifier circuit diagram is shown in Fig. 3. Integrated circuit operational amplifiers, IC_1 and IC_2, are coupled as voltage followers. This scheme results in a very high input impedance. The input cable shields have been bootstrapped to the respective voltage follower outputs to prevent the necessary input cable shielding from increasing the input capacity to an unacceptable value. This method is commonly used in ECG and EEG measurements.[3,4] The amplifiers used were all of the internal phase compensated type. These have an on-the-chip 30 pF capacitor, which is coupled to establish a Miller effect induced rolloff at −6 dB/octave down to unity gain.[5,6] No instability was observed, even when long bootstrapped cables were used.

The integrated circuit operational amplifier IC_3 is coupled as a differential input, gain of 50 amplifier. The over-all common mode rejection ability of the preamplifier

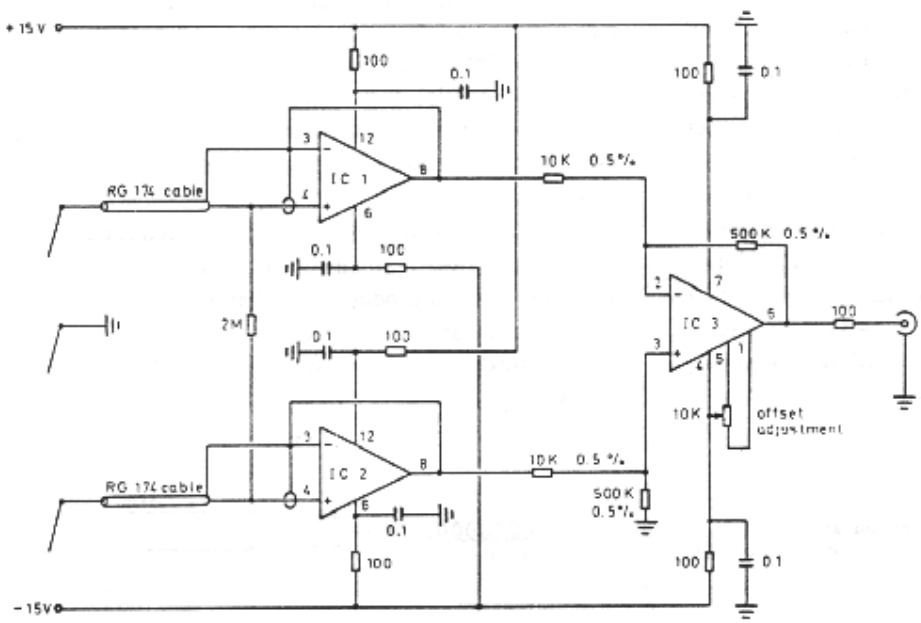

FIG. 3. The preamplifier circuit diagram. The pin numbers shown on IC_1, IC_2, and IC_3 correspond to the type C preamplifiers where $IC_1 = IC_2$ = Amelco 2741CF and IC_3 = MC1741CG, N5556T, μA741, or MC1456CG. All capacitors are low inductance disk type. In preamplifier type A, $IC_1 = IC_2 = IC_3$ = MC1741CG and in type B, $IC_1 = IC_2$ = N5556T and IC_3 = MC1741CG.

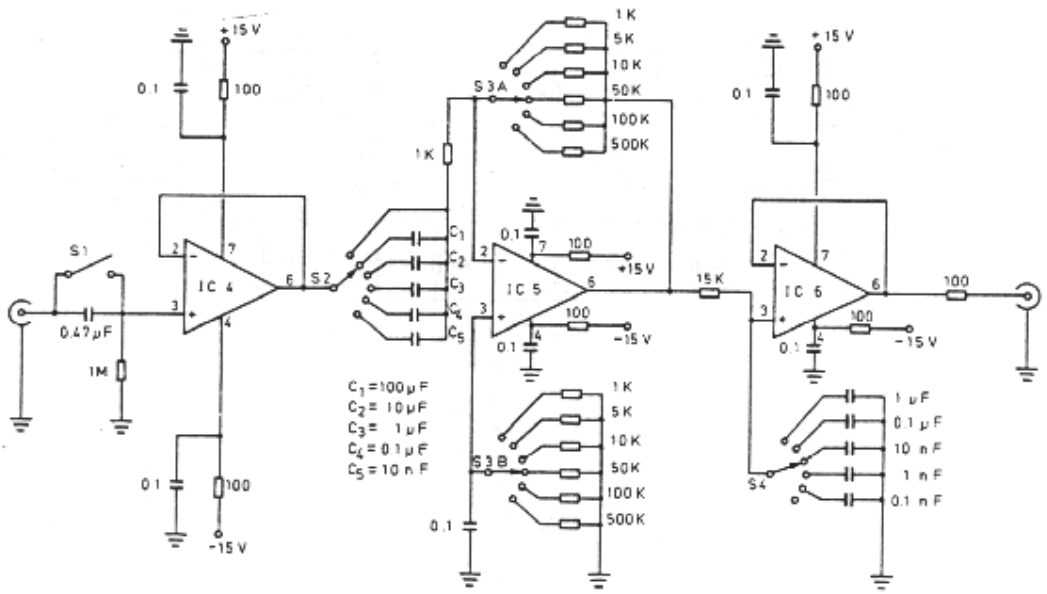

FIG. 4. The linear bandpass amplifier circuit diagram. $IC_4 = IC_5 = IC_6 = MC1741CG$ or $\mu A741$.

is mainly determined by four factors, the source impedance unbalance, the gain unbalance in IC_1 and IC_2, the lack of symmetry of the gain setting resistor network, and gain differences in the noninverting and the inverting gain path in IC_3.[7,8] Source impedance unbalance was found to be the dominant of these factors in the present application.

The linear band pass amplifier circuit diagram is shown in Fig. 4. Isolation of the high pass filter from the input is obtained by the operational amplifier IC_4 which is coupled as a voltage follower. The circuits IC_4, IC_5, and IC_6 are operational amplifiers of the $\mu A741$ type. The variable gain amplification is performed by IC_5. In order to decrease output dc level shifts as a result of gain shifting the resistor network connected to S_{3B} has been included.

The lower cutoff frequencies, chosen by the switch S_2, are 0, 1.6, 16, and 160 Hz, and 1.6 and 16 kHz. The upper −3 dB frequencies as selected by the switch S_4 are the following: 10 Hz, 100 Hz, 1, 10, and 100 kHz, and 1 MHz. The over-all passband characteristic of the linear amplifier is also determined by the frequency response capabilities of the $\mu A741$ amplifiers, in particular the gain providing IC_5 circuit. With a gain of 500, the upper −3 dB frequency for this amplifier is 5 kHz due to the −6 dB/octave rolloff, starting at 10 Hz, built into the $\mu A741$.[5]

ELECTRODES

Tests were carried out on two types of electrode material, gold and stainless steel. Metal electrodes were used because of their simplicity and low noise operation,[9] referring to what has been found to be the case in the field of animal electrophysiology. The gold electrodes were found superior to the stainless steel electrodes with regard to noise and the stability of the electrode–tissue interface potentials. Most probably a more suitable material than gold exists, but to investigate this was considered to be beyond the scope of the present investigations. With gold electrodes and the FET-input amplifiers, the electrode–tissue interface potentials became stable some 1–2 h after inserting the electrodes in the plant tissue. After stabilization, an interface potential drift of less than 1 mV per day and a peak-to-peak noise of less than 4 μV in the 1–50 Hz passband was measured with bias currents in the 100 pA range.

In Fig. 5 is shown the connection between the electrodes and the coax cables. Small coils made from 0.1 mm copper wire were used to produce a mechanical isolation between the coax cable and the electrodes. In this way only a minimum of force is exerted upon the electrodes by the coax cables.

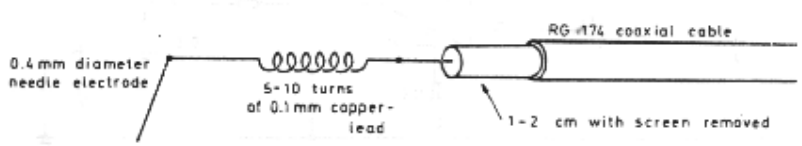

FIG. 5. The electrode-to-coax cable connection arrangement used to avoid mechanically loading the electrodes.

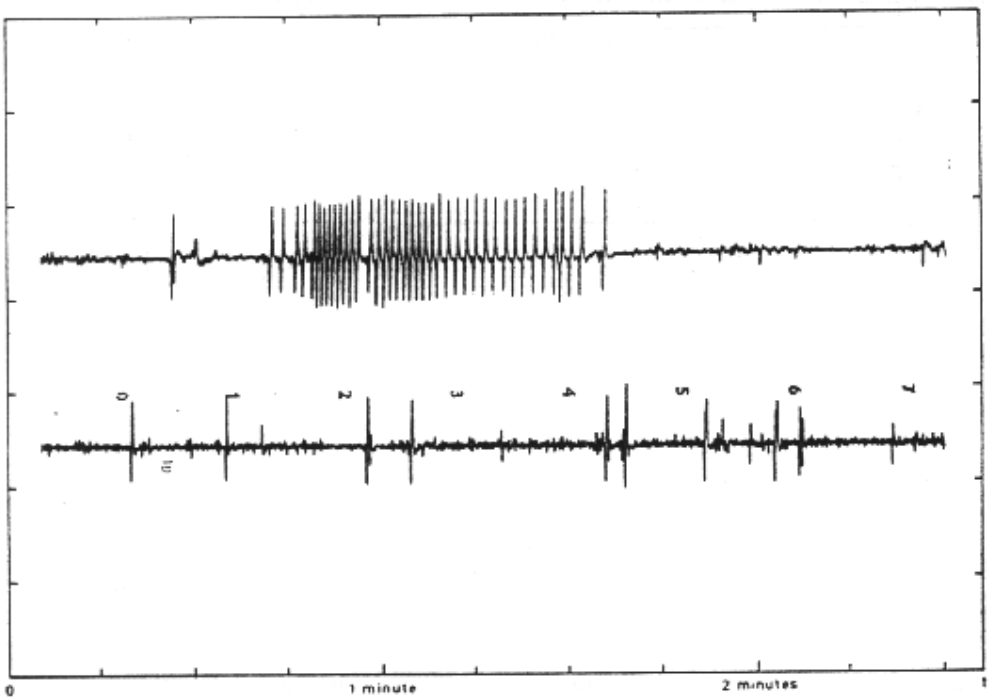

FIG. 6. A two channel simultaneous recording made by the experimental setup shown in Fig. 1. The vertical scale has a sensitivity of 80 μV/div. Note the excellent isolation between the channels.

CONSTRUCTION

The preamplifiers were built in metal boxes measuring 14×7×4 cm. Dual sided printed circuit was used throughout, with one side used solely as a ground plane. In this way the risk of instabilities due to poor decoupling is decreased. The input cables were connected via BNC connectors, which were mounted insulated from the metal box by means of nylon bushings. As shown in the circuit diagram (cf. Fig. 3), input guarding of the noninverting input terminal was used to prevent leakage currents in the printed circuit from producing input error signals.[7]

EXPERIMENTAL RESULTS

In Fig. 6 is shown a recording obtained with the experimental setup shown in Fig. 1. The bias currents I_{b1}, I_{b2}, I_{b3}, and I_{b4} were all less than 100 pA.

The common mode rejection capability of the preamplifiers was measured with the setup shown in Fig. 7. The resistor R_u was inserted in order to simulate the real part of the source impedance unbalance which can be present at the electrode–tissue interfaces. In Fig. 8 is shown the CMRR versus frequency as measured on a type C preamplifier equipped with two Amelco 2741 and one Signetics N5556 T operational amplifiers. Curve A represents the situation where the gain determining resistor network is made as shown in Fig. 3. Optimizing the value of the resistor from pin 3 on IC_3 to ground by means of a 470 kΩ resistor in series with a 100 kΩ trimpot, trimmed to a maximum of common mode signal rejection at 50 Hz, gave the CMRR shown by curve B. In order to improve the CMRR at higher frequencies, a 2–10 pF trim capacitor was inserted in parallel with one of the 500 kΩ resistors and trimmed to optimum performance at 50 kHz. The result of this is shown by curve C in Fig. 8 which displays an improvement of the CMRR at 50 kHz of about 20 dB. The correct position of the trim capacitor, of the two possible, is determined by trial because the function of this capacitor is to compensate for high fre-

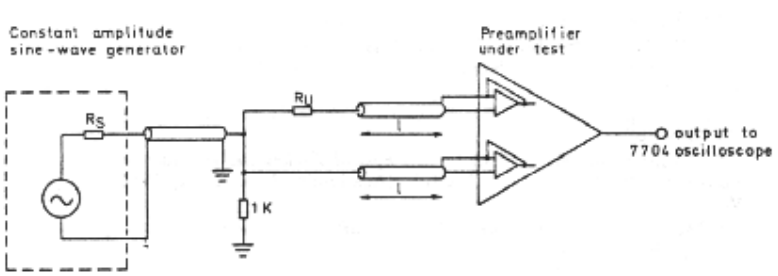

FIG. 7. A simplified circuit diagram of the setup used to measure the CMRR of the preamplifiers. The influence of the common mode signal amplitude on the CMRR is discussed in the text. The resistor R_u represents the source impedance unbalance.

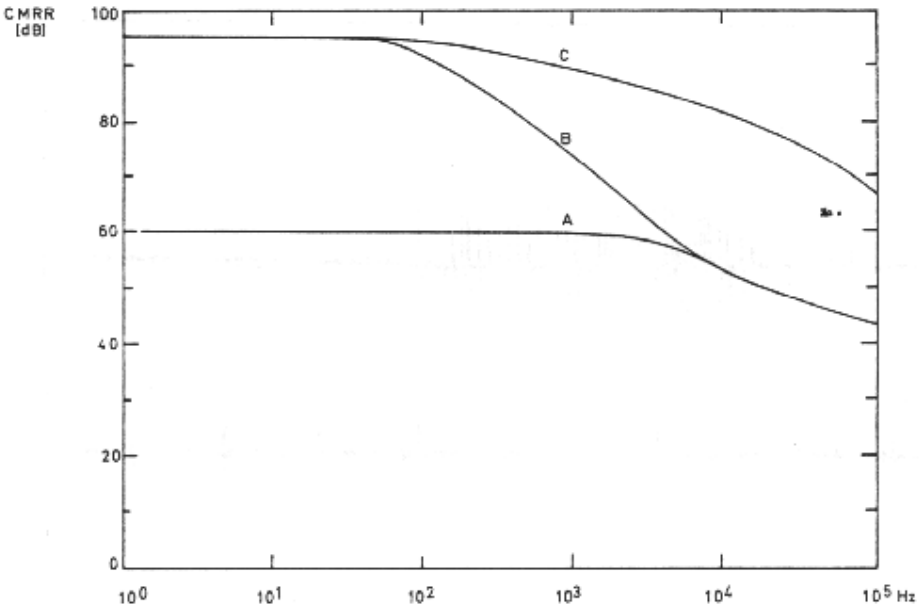

FIG. 8. Curves displaying the common mode rejection ratio versus frequency in the range from 1 Hz to 100 kHz. This was measured with a common mode signal amplitude of 1V, peak-to-peak, and with R_u equal to zero. See text about conditions adhering to A, B, and C.

quency gain and phase differences originating, primarily, in the IC_3 gain paths and the wiring layout used.

The CMRR measurements were made with a common mode signal amplitude of 1 V, which is representative of the amplitudes to be found in an actual measurement situation. Increasing the common mode signal amplitude from 1 to 10 V at 50 Hz resulted in a modest decrease in the CMRR from 94 to 82 dB.

The decrease in CMRR due to various degrees of source impedance unbalance was measured by varying the value of the resistor R_u, cf. Fig. 7. The results of these measurements are displayed graphically in Fig. 9. From this it is seen that the CMRR at 50 Hz decreases only moderately with increasing source impedance unbalance. The parameter l indicates the length of the input coax cables. At the higher frequencies this length has influence on the CMRR due to the nonzero input capacity of the bootstrapped preamplifier input. This implies that it is advantageous to keep the input coax cables as short as the experimental conditions allow.

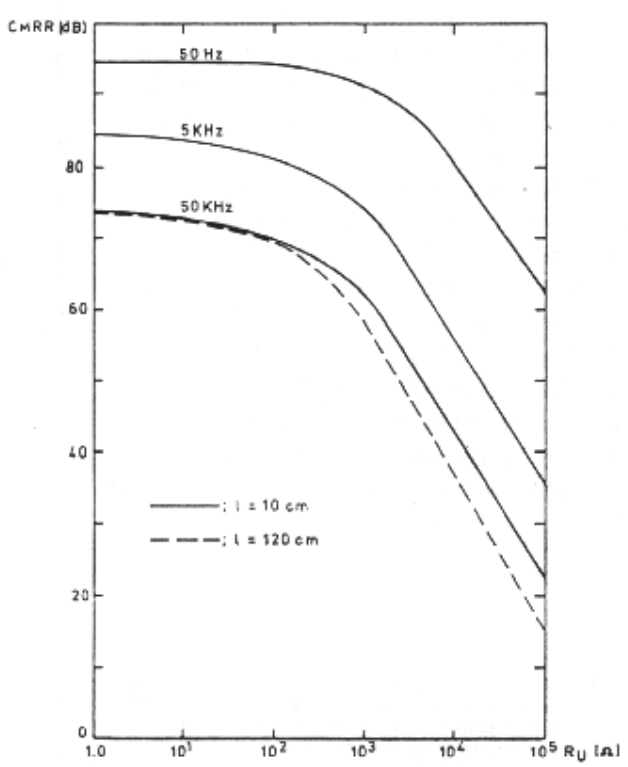

FIG. 9. Showing the observed CMRR degrading due to the real part of the source impedance unbalance measured with R_u values in the 0–100 kΩ range.

ACKNOWLEDGMENTS

The assistance of N. Cortsen in the development and construction of the instrumentation is gratefully acknowledged. The author is further indebted to members of the laboratory for support and encouragement.

[1] L. Karlsson, Plant Physiol. (to be published).

[2] J. W. Moore and K. S. Cole, in *Physical Techniques in Biological Research*, edited by W. L. Nastuk 1963, (Academic, New York, 1963), Vol. 6, Part B, p. 293.

[3] P. Strong, *Biophysical Measurements* (Tektronix, Beaverton, Ore., 1971), p. 302.

[4] K. Frank and M. C. Becker, in *Physical Techniques in Biological Research*, edited by W. L. Nastuk (Academic, New York, 1964), Vol. 5, Part A, p. 67.

[5] *The Application of Linear Microcircuits* (SGS Semiconductors, Milan, 1969), Vol. 2, p. 19.